NUMERIČKA SIMULACIJA DVOFAZNOG STRUJANJA SA MEĐUFAZNOM POVRŠINOM

NUMERICAL SIMULATION OF TWO-PHASE INTERFACIAL FLOWS

Edin Berberović

Polytechnic Faculty
University of Zenica

Ključne riječi:
numerička simulacija,
dvofazno strujanje,
metoda volumena fluida

Keywords:
numerical simulation,
two-phase flow
volume-of-fluid method

Paper received:
xx.xx.xxxx.
Paper accepted:
xx.xx.xxxx.

Stručni rad

REZIME

U radu se predstavlja volume-of-fluid (VOF) metod za praćenje međufazne površine u toku sa slobodnom površinom u softveru OpenFOAM®. VOF-model koristi algebarsku kompresivnu shemu za efektno sužavanje tranzicionog područja između tečne i gasovite faze. Podobnosti modela demonstriraju se simulacijom dvodimenzionalnog aksisimetričnog razvoja oblika kapljice u bezgravitacionoj okolini, kao i udara kapljice u tečni film na ravnom zidu. Uvidom u rezultate model daje dobre performanse za proračun dvofaznih tokova.

Professional paper

SUMMARY

The paper presents the volume-of-fluid (VOF) method for interface capturing in free surface flows in OpenFOAM® software. The VOF-model utilises an algebraic compressive scheme to effectively shrink the transitional region between the liquid and the gaseous phase. The capabilities of the model are demonstrated by simulating two-dimensional axisymmetric droplet shape evolution in a gravity-free environment, as well as drop impact on a liquid film at the flat wall. By inspection of results the model yields good performance for the computation of free-surface flows.

1. INTRODUCTION

Intensive and increased development of computers and computing power and efficiency have led to wider use of numerical methods in computations of free-surface flows. Numerical simulations are used to obtain a detailed insight into the dynamics of such flows with an amount of information which is experimentally and theoretically unachievable. Free-surface flows are important in many applications, such as ink-jet printing, paint spraying, internal combustion engines and spray cooling. These flows are very complex and there is ongoing research in developing models capable of computing them [1,2,3]. In the present paper the algebraic compressive VOF-model for interface capturing in computations of free-surface flows in the open-source CFD software OpenFOAM®[4] is presented.

2. COMPUTATIONAL MODEL

The main feature of the VOF-model is the motion of two incompressible immiscible fluids being modelled as a single effective fluid, the physical properties of which are weighted averages between the properties of each of fluids

1. UVOD

Intenzivan i ubrzan razvoj računara i računarske snage i efikasnosti doveli su do široke primjene numeričkih metoda u proračunima tokova sa slobodnim površinama. Numeričke simulacije se koriste za dobijanje detaljnog uvida u dinamiku takvih tokova uz ogromnu količinu informacija koje su nedostupne eksperimentalno i teorijski. Tokovi sa slobodnim površinama su važni u mnogim primjenama, kao što su ink-jet štampanje, lakiranje sprejem, motori sa unutrašnjim izgaranjem i hlađenje sprejem. Ovi tokovi su veoma kompleksni, pa su u toku istraživanja za razvoj modela za njihovo računanje [1,2,3]. U ovom radu predstavlja se algebarski kompresivni VOF-model za praćenje međufazne površine u proračunu toka sa slobodnom površinom u open-source CFD softveru OpenFOAM®[4].

2. RAČUNARSKI MODEL

Glavna osobina VOF-modela je da se kretanje dva nestišljiva nemiješajuća fluida modelira kao kretanje jednog efektivnog fluida, čije fizikalne osobine predstavljaju težinski usrednjene vrijednosti osobina svakog pojedinačnog fluida,

depending on the distribution of the phase fraction and being equal to the properties of pure fluids in regions they occupy and varying only across the interface. The free surface is tracked by using the phase fraction γ of one of the fluids, commonly of the liquid, which takes values between 1 and 0.

2.1. Governing equations

The mathematical model for the free-surface flow consists of the governing transport equations for the conservation of mass, phase fraction and momentum in the following form

$$\nabla \cdot \mathbf{U} = 0, \tag{1}$$

$$\frac{\partial \gamma}{\partial t} + \nabla \cdot \left(\mathbf{U} \gamma \right) + \nabla \cdot \left[\mathbf{U}_c \gamma \left(1 - \gamma \right) \right] = 0, \tag{2}$$

$$\frac{\partial \left(\rho \mathbf{U} \right)}{\partial t} + \nabla \cdot \left(\rho \mathbf{U} \mathbf{U} \right) = -\nabla p_d + \nabla \cdot \left(\mu \nabla \mathbf{U} \right) + \nabla \mathbf{U} \cdot \nabla \mu - \mathbf{g} \cdot \mathbf{x} \nabla \rho + \sigma \kappa \nabla \gamma, \tag{3}$$

where $\mathbf{U}$ is the velocity of the effective fluid, γ is the phase fraction, ρ and μ are the density and viscosity of the effective fluid, p_d is the modified pressure obtained by absorbing the hydrostatic contribution into the pressure, $\mathbf{x}$ is the position vector, $\mathbf{g}$ is acceleration due to gravity, σ is the surface tension coefficient and κ is the curvature of the interface. The last term in Eq. (3) is the Continuum Surface Force model for the surface tension [5]. Fluid properties are calculated as weighted averages: e.g. some property y of the effective fluid is $y = \gamma y_l + \left(1 - \gamma \right) y_g$. The free-surface curvature is calculated as $\kappa = -\nabla \cdot \left(\nabla \gamma / \left| \nabla \gamma \right| \right)$. The additional convective term in Eq. (2) is the so-called compressive term which is active only in the interface region and serves the purpose of effectively shrinking the smeared interface and provide a sharp interface representation in the simulation [6].

2.2. Details of the computational model

The model is implemented in OpenFOAM® [4] utilizing the finite volume method for arbitrary unstructured meshes, Fig. 1. In the discretization and integration of the model Eqns. (1)-(3) the integrals are evaluated by using the mid-point rule and the time derivatives by using the implicit Euler scheme. The spatial derivatives are calculated as surface integrals by using Gauss's theorem. Convective terms are calculated using the Gamma differencing scheme [7].

u zavisnosti od raspodjele faznog udjela, te su jednake osobinama čistih fluida u područjima koje oni zauzimaju, a mijenjaju se samo preko međufazne površine. Slobodna površina se prati korištenjem faznog udjela γ jednog od fluida, obično tečnosti, a koji može uzimati vrijednosti između 1 i 0.

2.1. Jednačine modela

Matematski model za tok sa slobodnom površinom sastoji se od osnovnih jednačina za konzervaciju mase, faznog udjela i količine kretanja, u slijedeće, obliku

$$\nabla \cdot \mathbf{U} = 0, \tag{1}$$

$$\frac{\partial \gamma}{\partial t} + \nabla \cdot \left(\mathbf{U} \gamma \right) + \nabla \cdot \left[\mathbf{U}_c \gamma \left(1 - \gamma \right) \right] = 0, \tag{2}$$

$$\frac{\partial \left(\rho \mathbf{U} \right)}{\partial t} + \nabla \cdot \left(\rho \mathbf{U} \mathbf{U} \right) = -\nabla p_d + \nabla \cdot \left(\mu \nabla \mathbf{U} \right) + \nabla \mathbf{U} \cdot \nabla \mu - \mathbf{g} \cdot \mathbf{x} \nabla \rho + \sigma \kappa \nabla \gamma, \tag{3}$$

gdje je $\mathbf{U}$ brzina efektivnog fluida, γ je fazni udio, ρ i μ su gustina i viskoznost efektivnog fluida, p_d je modificirani pritisak koji se dobija apsobiranjem hidrostatičkog udjela u pritisak, $\mathbf{x}$ je vektor položaja, $\mathbf{g}$ vektor ubrzanja Zemljine teže, σ je koeficijent površinskog napona i κ je zakrivljenost međufazne površine. Zadnji član u jednačini (3) je Continuum Surface Force model za površinski napon [5]. Osobine fluida se računaju kao težinske srednje vrijednosti: npr. neka osobina y efektivnog fluida je $y = \gamma y_l + \left(1 - \gamma \right) y_g$. Zakrivljenost slobodne površine računa se kao $\kappa = -\nabla \cdot \left(\nabla \gamma / \left| \nabla \gamma \right| \right)$. Dodatni konvektivni član u jednačini (2) je tzv. kompresivni član, koji je aktivan samo na međufaznoj površini i služi za efektivno sužavanje razmazane međufazne površine i daje oštru reprezentaciju međufazne površine u simulaciji [6].

2.2. Detalji računarskog modela

Model je implementiran u softver OpenFOAM® [4] koji koristi metod konačnih zapremina na proizvoljnim nestrukturiranim mrežama, slika 1. Kod diskretizacije i integracije modelskih jednačina (1)-(3) integrali se računaju korištenjem pravila srednje vrijednosti, a vremenski izvodi korištenje implicitne sheme Euler. Prostorni izvodi se računaju kao površinski integrali pomoću Gaussove teoreme. Konvektivni članovi se računaju pomoću Gamma sheme diferenciranja [7].

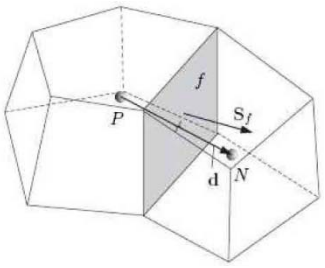

Slika 1. *Diskretizacija domene rješavanja [4]*
Figure 1. *Discretization of solution domain [4]*

The compression velocity $\mathbf{U}_c$ in Eq. (2) is related to the maximum velocity in the solution domain and modelled as

$$\mathbf{U}_c = \min\left[C_\gamma |\mathbf{U}|, \max\left(|\mathbf{U}|\right)\right]\nabla\gamma / |\nabla\gamma|. \quad (4)$$

The intensity of the interface compression is controlled by the parameter C_γ: there is no compression for C_γ =0, conservative compression for C_γ =1, and enhanced compression for C_γ>1 [6]. The cell-face volume flux in the integration of Eq. (2) arises from the pressure-velocity coupling algorithm

$$\left|\mathbf{U}_{c,f}\cdot\mathbf{S}_f\right| = n_f \min\left[C_\gamma \frac{\left|\mathbf{U}\cdot\mathbf{S}_f\right|}{\left|\mathbf{S}_f\right|}, \max\left(\frac{\left|\mathbf{U}\cdot\mathbf{S}_f\right|}{\left|\mathbf{S}_f\right|}\right)\right], \quad (5)$$

where $\left|\mathbf{U}\cdot\mathbf{S}_f\right|$ is the cell-face volume flux, and n_f is the face unit normal flux, calculated from phase fraction gradients at cell-faces

$$n_f = \frac{(\nabla\gamma)_f}{\left|(\nabla\gamma)_f\right| + \delta_n}\cdot\mathbf{S}_f. \quad (6)$$

The stabilization factor used in the normalisation of the phase fraction gradient is evaluated as

$$\delta_n = \varepsilon / \left(\sum_{i=1}^{N} V_i / N\right)^{1/3}, \quad (7)$$

where N is the number of computational cells and ε is a small value set to 10^{-8}.

2.3. Time-step adjustment

The time step is adjusted within the time loop according to the maximum prescribed Courant number, which is usually set to Co_{max}=0.2. The new time step is evaluated from the expression

Brzina kompresije $\mathbf{U}_c$ u jednačini (2) izražava se u odnosu na maksimalnu brzinu u proračunskoj domeni i modelira se kao

$$\mathbf{U}_c = \min\left[C_\gamma |\mathbf{U}|, \max\left(|\mathbf{U}|\right)\right]\nabla\gamma / |\nabla\gamma|. \quad (4)$$

Intenzitet kompresije međufazne površine kontroliše se parametrom C_γ: ne postoji kompresija za C_γ =0, kompresija je konzervativna za C_γ=1, a povećana kompresija je za C_γ > 1 [6]. Volumni fluks na površinama ćelija u integraciji jednačine (2) se dobija iz algoritma za kuplovanje pritisak-brzina

$$\left|\mathbf{U}_{c,f}\cdot\mathbf{S}_f\right| = n_f \min\left[C_\gamma \frac{\left|\mathbf{U}\cdot\mathbf{S}_f\right|}{\left|\mathbf{S}_f\right|}, \max\left(\frac{\left|\mathbf{U}\cdot\mathbf{S}_f\right|}{\left|\mathbf{S}_f\right|}\right)\right], \quad (5)$$

gdje je $\left|\mathbf{U}\cdot\mathbf{S}_f\right|$ volumni fluks na površini ćelije, a n_f je jedinični fluks normale na površinu, koji se računa iz gradijenta faznog udjelana površini

$$n_f = \frac{(\nabla\gamma)_f}{\left|(\nabla\gamma)_f\right| + \delta_n}\cdot\mathbf{S}_f. \quad (6)$$

Faktor stabilizacije koji se koristi u normalizaciji gradijenta faznog udjela računa se kao

$$\delta_n = \varepsilon / \left(\sum_{i=1}^{N} V_i / N\right)^{1/3}, \quad (7)$$

gdje je N broj računskih ćelija, a ε je mala vrijednost postavljena na 10^{-8}.

2.3. Prilagođavanje vremenskog koraka

Vremenski korak se prilagođava unutar vremenske petlje prema maksimalnom zadanom Courantovom broju, obično Co_{max}=0.2. Novi vremenski korak se računa iz izraza

$$\Delta t^{n*} = \min\left\{\begin{matrix}\dfrac{\mathrm{Co}_{\max}}{\mathrm{Co}^o}\Delta t^o, \lambda_2\Delta t^o, \Delta t_{\max} \\ \left(1+\lambda_1\dfrac{\mathrm{Co}_{\max}}{\mathrm{Co}^o}\right)\Delta t^o,\end{matrix}\right\}, \quad (8)$$

based on the value for the Courant number Co

$$\mathrm{Co} = \Delta t\left|\mathbf{U}_f\cdot\mathbf{S}_f\right| / \left(\mathbf{d}\cdot\mathbf{S}_f\right), \quad (9)$$

where ***d*** is the vector connecting two adjacent cell-centers in the mesh. The maximum local Co number, Co^o, is calculated using values from previous time step, and Δt_{max} and Co_{max} are the prescribed limit values for the time step and Courant number. In order to avoid time step oscillations, the increase of the time step is damped using factors λ_1 and λ_2. For the solution to be stored at exactly specified times, the output is adjusted by calculating the number of time steps remaining to next write n_{nw}, rounded to the first greater integer value

$$n_{nw} = INT\left[\frac{\left(i_{t,out}+1\right)\Delta t_{wr} - \left(t-t_0\right)}{\Delta t^{n*}} - \varepsilon_t + 1\right] \quad (10)$$

where $i_{t,out}$ is the output time index indicating how many times the solution was stored, Δt_{wr} is the specified write interval, t and t_0 are current and initial time, and $\varepsilon_t=10^{-15}$ is the prescribed tolerance used to avoid adding one time step if the value of the fraction on the r.h.s. of Eq. (8) is greater than but close to integer value within the tolerance. The new time step is then evaluated as

$$\Delta t^{n**} = \left[\left(i_{t,out}+1\right)\Delta t_{wr} - \left(t-t_0\right)\right] / n_{nw}. \quad (11)$$

Since the value obtained from Eq. (11) may differ from that in Eq. (8), to avoid instability an additional control of the decrease and increase of the time step is provided, yielding the final expression for the new time step

$$\Delta t^{n} = \begin{cases}\min\left(\Delta t^{n**}, 2\Delta t^{n*}\right), & \text{for } \Delta t^{n**} \geq \Delta t^{n*} \\ \max\left(\Delta t^{n**}, 0.2\Delta t^{n*}\right), & \text{for } \Delta t^{n**} < \Delta t^{n*}\end{cases} \quad (12)$$

2.4. Time sub-cycling and source-term reconstruction

The phase fraction equation is solved in several subcycles within a single time step. The value of

$$\Delta t^{n*} = \min\left\{\begin{matrix}\dfrac{\mathrm{Co}_{\max}}{\mathrm{Co}^o}\Delta t^o, \lambda_2\Delta t^o, \Delta t_{\max} \\ \left(1+\lambda_1\dfrac{\mathrm{Co}_{\max}}{\mathrm{Co}^o}\right)\Delta t^o,\end{matrix}\right\}, \quad (8)$$

zavisno od vrijednosti Courantovog broja Co

$$\mathrm{Co} = \Delta t\left|\mathbf{U}_f\cdot\mathbf{S}_f\right| / \left(\mathbf{d}\cdot\mathbf{S}_f\right), \quad (9)$$

gdje je ***d*** vector koji spaja dva susjedna centra ćelija u mreži. Maksimalni lokalni Co broj, Co^o, računa se korištenjem vrijednosti iz prethodnog vremenskog koraka, a Δt_{max} i Co_{max} su postavljene granične vrijednosti za vremenski korak i Courantov broj. Da bi se izbjegle oscilacije vremenskog koraka, njegov porast se prigušuje faktorima λ_1 i λ_2. Da bi se rješenje zapisivalo u tačno specificiranim vremenima, izlaz se prilagođava računanjem broja vremenskih koraka do narednog zapisa n_{nw}, zaokruženog na prvi veći cijeli broj

$$n_{nw} = INT\left[\frac{\left(i_{t,out}+1\right)\Delta t_{wr} - \left(t-t_0\right)}{\Delta t^{n*}} - \varepsilon_t + 1\right] \quad (10)$$

gdje je $i_{t,out}$ indeks vremena zapisa koji pokazuje koliko puta je rješenje bilo već zapisano, Δt_{wr} je zadani vremenski interval zapisa, t i t_0 su trenutno i početno vrijeme, a $\varepsilon_t=10^{-15}$ je tolerancija da bi se izbjeglo povećanje vremenskog koraka ako je razlomak na desnoj strani izraza (8) veći, ali vrlo blizu, cijelog broja unutar tolerancije. Novi vremenski korak je

$$\Delta t^{n**} = \left[\left(i_{t,out}+1\right)\Delta t_{wr} - \left(t-t_0\right)\right] / n_{nw}. \quad (11)$$

Vrijednost dobivena izrazom (11) može se razlikovati od one dobivene izrazom (8), pa se nestabilnost izbjegava dodatnom kontrolom smanjenja i povećanja vremenskog koraka, što daje konačan izraz za novi vremenski korak

$$\Delta t^{n} = \begin{cases}\min\left(\Delta t^{n**}, 2\Delta t^{n*}\right), & \text{for } \Delta t^{n**} \geq \Delta t^{n*} \\ \max\left(\Delta t^{n**}, 0.2\Delta t^{n*}\right), & \text{for } \Delta t^{n**} < \Delta t^{n*}\end{cases} \quad (12)$$

2.4. Vremenski podciklusi i rekonstrukcija izvornih članova

Jednačina za fazni udio rješava se u podciklusima u vremenskom koraku. Vrijednost

the sub-cycle time step is obtained by dividing the global time step by the preset number of sub-cycles and the total mass flux in the global time step is calculated by summing the sub-cycle mass fluxes. In the calculations of source terms in Eq. (3) the cell-center values are obtained by reconstructing them from the cell-face values as weighted averages. For example, the source coming from the pressure gradient in the momentum equation is calculated as

$$\left(\nabla p_d\right)_P = \left(\sum_f \frac{\mathbf{S}_f \mathbf{S}_f}{\left|\mathbf{S}_f\right|}\right)^{-1} \cdot \left(\sum_f \frac{\mathbf{S}_f}{\left|\mathbf{S}_f\right|} \cdot \left(\nabla p_d\right)_f\right) \quad (14)$$

The coupling between pressure and velocity is ensured by adopting the PISO algorithm [8]. The same reconstructing procedure is used for recovering velocities from conservative face fluxes in the corrector stage of the PISO algorithm.

3. RESULTS

The performance of the model is tested by computing the liquid droplet shape evolution in zero gravity and drop impact onto a liquid wall-film. The calculations are initialised by prescribing the distribution of phase fraction (and velocity for the case of drop impact). The set of boundary conditions for the case of drop impact consists of axis of symmetry, the no-slip condition at the wall and open top boundary. For the case of gravity-free droplet shape evolution the plane of symmetry is used instead of the bottom wall. Both cases are two-dimensional and axisymmetric. The physical properties of liquids are given in Table 1, and atmospheric air was used as the gaseous fluid.

vremenskog koraka u podciklusu dobija se dijeljenjem globalnog vremenskog koraka zadanim brojem podciklusa, a ukupni maseni fluks u globalnom vremenskom koraku računa se sumiranjem flukseva iz podciklusa. Za računanje izvornih članova u jednačini (3) vrijednosti u centrima ćelija dobijaju se težinskom rekonstrukcijom vrijednosti sa površina ćelija. Na primjer, gradijent pritiska u jednačini količine kretanja se računa kao

$$\left(\nabla p_d\right)_P = \left(\sum_f \frac{\mathbf{S}_f \mathbf{S}_f}{\left|\mathbf{S}_f\right|}\right)^{-1} \cdot \left(\sum_f \frac{\mathbf{S}_f}{\left|\mathbf{S}_f\right|} \cdot \left(\nabla p_d\right)_f\right) \quad (14)$$

Kuplovanje pritiska i brzine osigurava se izborom PISO algoritma [8]. Ista procedura rekonstrukcije koristi se za dobijanje brzina iz konzervativnih volumnih flukseva na površibnama ćelija u korektorskom koraku u PISO algoritmu.

3. REZULTATI

Mogućnosti modela testiraju se računanjem evolucije oblika kapljice u bezgravitacionom području, te udara kapljice u tečni film na zidu. Proračun se inicijalizira postavljanjem raspodjele faznog udjela (i brzine za slučaj udara kapljice). Set graničnih uslova za slučaj udara kapljice sastoji se od ose simetrije, uslova no-slip na zidu i otvorene granice s gornje strane. Za slučaj evolucije oblika kapljice u bezgravitacionom prostoru koristi se ravan simetrije umjesto graničnog uslova za donji zid. Oba slučaja su dvodimenzionalna i aksisimetrična. Fizikalne osobine tečnosti su date u tabeli 1, a kao gasoviti fluid koristi se atmosferski zrak.

Tabela 1. Fizikalne osobine fluida
Table 1. Physical properties of fluids

Case	Density ρ / kg/m^3	Viscosity μ / Pas	Surface tension σ / N/m
Gravity-free drop	805	$2.3 \cdot 10^{-3}$	$2.36 \cdot 10^{-2}$
Drop impact	1179	$7.1 \cdot 10^{-3}$	$6.68 \cdot 10^{-2}$
Air (both cases)	1.18	$1.82 \cdot 10^{-5}$	

3.1. Droplet shape evolution in zero gravity

In the case of the gravity-free droplet the liquid is initialised as the cylindrical section in two dimensions and the mesh has 100×100 cells. The computed interface shape at various times is shown in Fig. 2. The phase-interface is represented in colors for γ from 0.1 to 0.9.

3.1. Evolucija oblika kapljice bez gravitacije

U slučaju kapljice u bezgravitacionom prostoru tečnost se inicijalizira kao dio cilindra u dvije dimenzije i mreža ima 100×100 ćelija. Proračunom dobivena međufazna površina prikazana je na slici 2. Međufazna površina predstavljena je bojama za γ od 0.1 do 0.9.

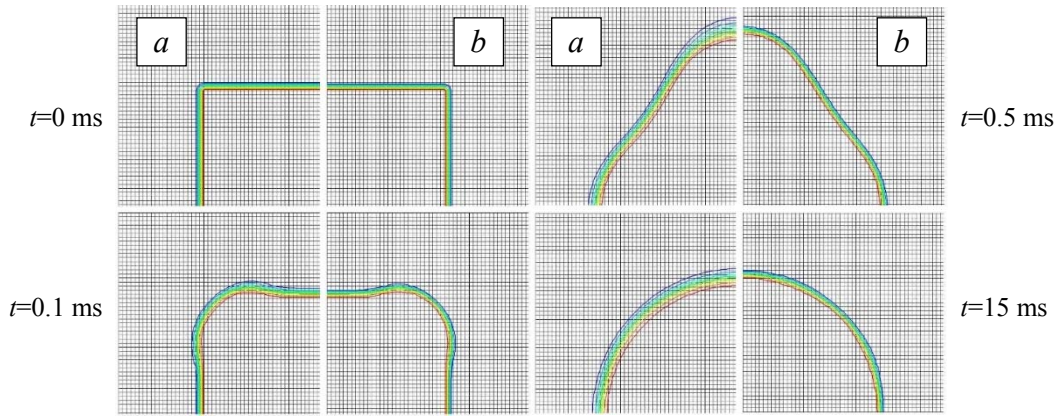

Slika 2. *Proračunom dobiven oblik međufazne površine bez (a) i sa kompresijom slobodne površine (b)*
Figure 2. *The computed interface shape evolution without (a) and with interface compression (b).*

It is seen that the interface is resolved more sharply with interface compression. Quantitative comparison is performed by evaluating the finite droplet radius from the theoretical equality of volumes of cylinder and sphere $R_{cyl}^2 \pi H = (4/3) R_{sph}^3 \pi$, yielding the theoretical droplet radius R_{sph}=0.3434 mm. The corresponding pressure drop across the spherical interface is

$$\Delta p = 2\sigma R_{sph} = 137.449 \text{ Pa} \ , \qquad (15)$$

which, in the absence of gravity, should be reached when the droplet becomes spherical.
The mean pressure within the droplet is calculated as a weighted average

$$p_d = \sum_{i=1}^{N} p_i V_i \Big/ \sum_{i=1}^{N} V_i \ , \qquad (16)$$

where N is the number of cells containing liquid with the criterion $\gamma \geq 0.99$ (≥99% liquid).
Values of the droplet radius are tracked in time in three planes: horizontal, vertical and at the angle of 45°. The representative interface-point is the first point satisfying the criterion $\gamma \geq 0.5$. The computed results are shown in Fig. 3. There is a small difference between the three values for the droplet radius indicating that the droplet in simulations is not perfectly spherical. Without interface compression the differences are greater and last longer time, which is attributed to more smeared interface. The greatest difference of the computed and theoretical radius is ≈0.96% for the model without and ≈0.81% with interface compression.

Vidi se da je međufazna površina oštrije izračunata korištenjem kompresije površine. Kvantitativno poređenje urađeno je računanjem konačnog radijusa kojeg kapljica ima na osnovu teorijske jednakosti volumena cilindra i sfere $R_{cyl}^2 \pi H = (4/3) R_{sph}^3 \pi$, što daje teorijski radijus kapljice R_{sph}=0.3434 mm. Odgovarajući pad pritiska preko međufazne površine sfernog oblika je

$$\Delta p = 2\sigma R_{sph} = 137.449 \text{ Pa} \ , \qquad (16)$$

koji, u odsustvu gravitacije, mora biti dostignut kada kapljica zauzme sferni oblik.
Srednji pritisak unutar kapljice računa se kao težinska srednja vrijesnost

$$p_d = \sum_{i=1}^{N} p_i V_i \Big/ \sum_{i=1}^{N} V_i \ , \qquad (16)$$

gdje je N broj ćelija koje sadrže tečnost uz kriterij $\gamma \geq 0.99$ (≥99% tečnosti).
Vrijednosti radijusa kapljice se prate u vremenu u tri ravni: horizontalnoj, vertikalnoj i pod uglom od 45°. Reprezentativna tačka na međufaznoj površini je prva tačka koja zadovoljava uslov $\gamma \geq 0.5$. Proračunom dobiveni rezultati prikazani su na slici 3. Postoji mala razlika između tri vrijednosti za radijus kapljice, što ukazuje na to da kapljica u simulaciji nije idealnog sferičnog oblika. Bez kompresije međufazne površine ove razlike su veće i vremenski duže traju, zbog razmazane međufazne površine. Najveća razlika između računskog i teorijskog radijusa je ≈0.96% za model bez, a ≈0.81% za model sa kompresijom međufazne površine.

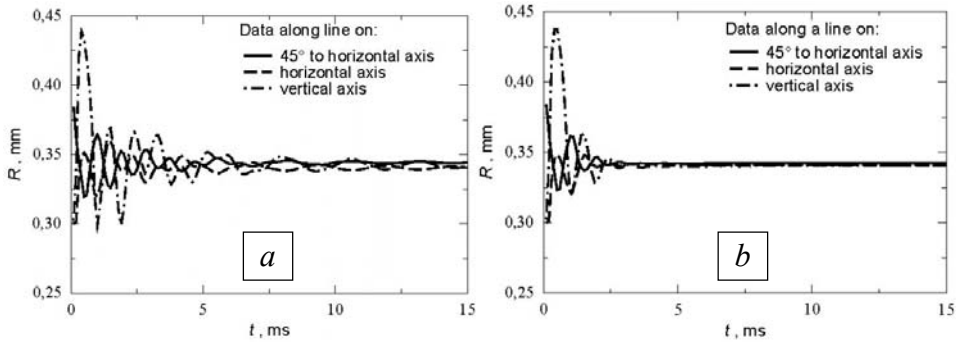

Slika 3. *Proračunata evolucija radijusa kapljice bez (a) i sa kompresijom slobodne površine (b)*
Figure 3. *The computed droplet radius evolution without (a) and with interface compression (b)*

The predicted pressure drop across the interface at t=15 ms is shown in Fig. 4. It is sharply predicted with interface compression, but with slightly lower value than the theoretical one. In order to investigate effects of the mesh resolution computations were performed using meshes with 50×50, 150×150, 200×200 and 250×250 cells. The results at time t=15 ms in Fig. 5 show no clear mesh dependence. The difference in pressure drop compared to the theoretical value is ≈1% for the model without, and ≈5% with interface compression.

Proračunom dobiveni pad pritiska preko međufazne površine u t=15 ms prikazan je na slici 4. Ovaj pad je oštar ako se koristi kompresija međufazne površine, ali je nešto manji od teorijskog. Za istraživanje uticaja rezolucije mreže urađeni su proračuni na mrežama sa 50×50, 150×150, 200×200 i 250×250 ćelija. Rezultati za t=15 ms na slici 5 ne daju jasnu zavisnost od mreže. Razlika u padu pritiska u odnosu na teorijski je ≈1% za model bez, a ≈5% za miodel sa kompresijom međufazne površine.

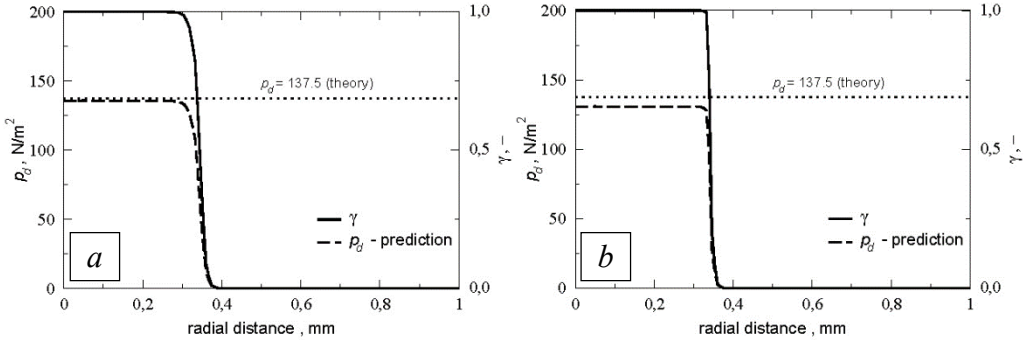

Slika 4. *Proračunom dobiveni pad pritiska bez (a) i sa kompresijom slobodne površine (b)*
Figure 4. *The computed pressure drop without (a) and with interface compression (b)*

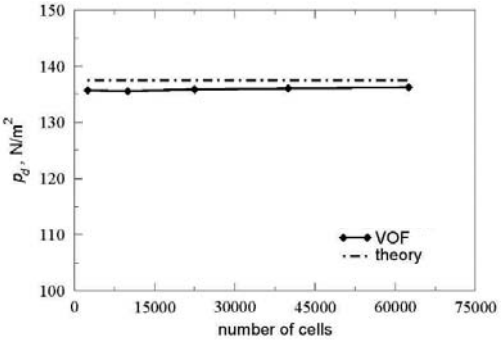

Slika 5. *Pad pritiska dobiven proračunom sa različitim mrežama*
Figure 5. *The computed pressure drop obtained on different meshes*

The computed velocity fields are shown in Fig. 6 at the time where some bulk motion of the liquid

Proračunom dobiveno polje brzine dato je na slici 6 u trenutku kad još postoji kretanje tečnosti

still exists and at time t=15 ms when the droplet has reached the quasi-equilibrium shape. It is seen that when the bulk velocity is close to zero, the generated parasitic currents are less in the model with interface compression.

i u trenutku t=15 ms u kojem je kapljica dostigla svoj kvazi-ravnotežni oblik. Vidi se da, kada je brzina kretanja blizu nule, generirane parazitske struje su manje kod modela sa kompresijom međufazne površine.

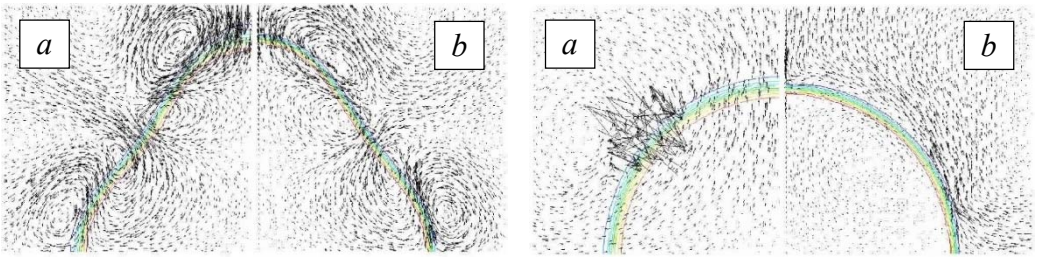

Slika 6. *Proračunom dobivena polja brzine bez (a) i sa kompresijom slobodne površine (b)*
Figure 6. *The computed velocity fields without (a) and with interface compression (b).*

3.2. Drop impact onto a wall-film

For the case of drop impact the liquid in the drop is initialised as the spherical section and the wall-film as the cylindrical section in two dimensions. The mesh is refined in the region of impact with about 70 000 cells, Fig. 7.

3.2. Udar kapljice na tečni film

Za slučaj udara kapljice tečnost u kapljici se inicijalizira kao dio sfere, a film na zidu kao dio cilindra u dvije dimenzije. Mreža je ufinjena u području u kojem se dešava udar i ima oko 70 000 ćelija, slika 7.

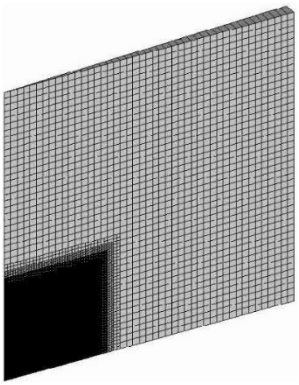

Slika 7. *Računska mreža za proračun udara kapljice*
Figure 7. *The computational mesh for the drop impact case*

The sequence of stages after the impact is described in experiments in [9]. Upon the first contact, a small circumferential liquid jet is ejected upward, a crater is formed in the wall film which expands, then recedes due to surface tension effects and collapses ejecting a jet in upward direction. The computed interface shape at various times is shown in Fig. 8. The interface is rather smeared without interface compression which eventually leads to a nonphysical solution at later times. The results are quantitatively evaluated by using the predicted crater diameter and depth. The crater depth is determined by using the phase fraction $\gamma \geq 0.1$, $\gamma \geq 0.5$ and $\gamma \geq 0.9$ at the axis of symmetry. The crater diameter is determined at the half film depth using the same criteria.

Redoslijed dešavanja nakon udara opisan je u eksperimentima u [9]. Nakon prvog kontakta izbacuje se mali tečni mlaz po obimu naviše, formira se krater u filmu na zidu, koji se širi, a potom smanjuje pod uticajem površinskog napona i kolabira izbacujući mlaz vertikalno naviše. Proračunom dobiveni oblici međufazne površine u toku vremena dati su na slici 8. Bez primjene kompresije, međufazna površina je prilično razmazana, što u konačnici dovodi do nefizikalnog rješenja u kasnijem vremenu. Rezultati se kvantitativno procjenjuju korištenjem prečnika i dubine kratera. Dubina kratera se određuje korištenjem faznog udjela $\gamma \geq 0.1$, $\gamma \geq 0.5$ and $\gamma \geq 0.9$ na osi simetrije. Prečnik kratera se određuje na polovini dubine tečnog filma za isti kriterij.

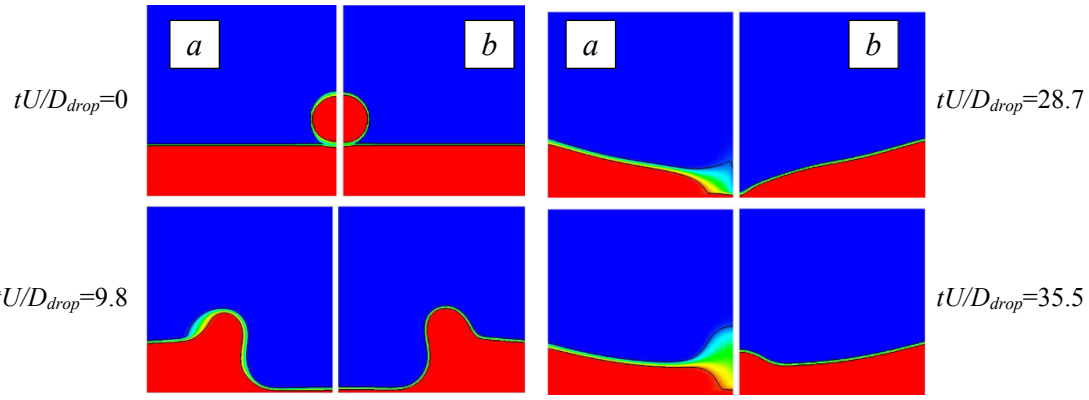

Slika 8. *Proračunom dobiven udar kapljice na tečni film bez (a) i sa kompresijom slobodne površine (b)*
Figure 8. *The computed drop impact onto a wall film without (a) and with interface compression (b)*

The computed results for the crater diameter and depth vs. time are shown in Fig. 9 and Fig. 10. The results without interface compression are different and only the value $\gamma \geq 0.1$ yields good agreement for the crater depth, but with this value the crater diameter is rather underestimated. On the other hand, the interface compression yields good results for crater diameter and depth. The change of the time step size and the corresponding number of iterations vs. run time is shown in Fig. 11. The size of the time step is varying between the orders of 10^{-7} and 10^{-5}, thus the adaptive time step considerably reduces the simulation time.

Proračunom dobiveni rezultati za prečnik i dubinu kratera u vremenu prikazani su na slikama 9 i 10. Rezultati dobiveni bez kompresije međufazne površine su različiti, a samo vrijednost $\gamma \geq 0.1$ daje dobro slaganje za dubinu kratera, ali sa ovom vrijednošću prečnik kratera je prilično podračunat. S druge strane, kompresija međufazne površine daje daje dobre rezultate za prečnik i dubinu kratera. Promjena vremenskog koraka i odgovarajući broj iteracija u vremenu dati su na slici 11. Vremenski korak varira između reda veličine 10^{-7} i 10^{-5}, pa prilagođavanje vremenskog koraka značajno smanjuje vrijeme trajanja simulacije.

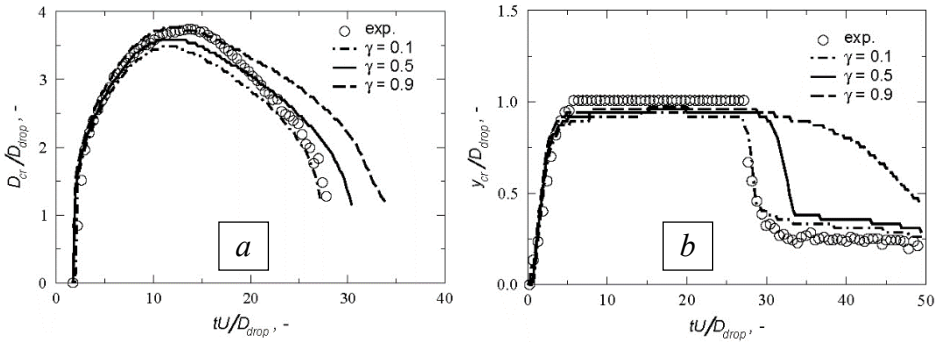

Slika 9. *Poračunom dobiveni prečnik (a) i dubina kratera (b), bez kompresije slobodne površine*
Figure 9. *The computed crater diameter (a) and depth (b), without interface compression*

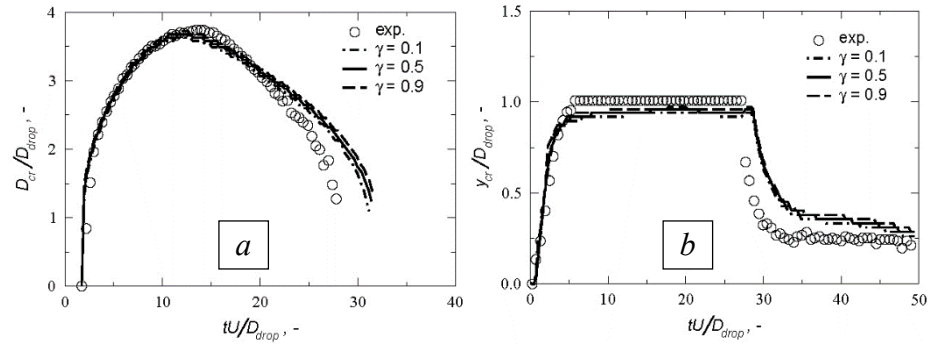

Slika 10. *Poračunom dobiveni prečnik (a) i dubina kratera (b), sa kompresijom slobodne površine*
Figure 10. *The computed crater diameter (a) and depth (b), with interface compression*

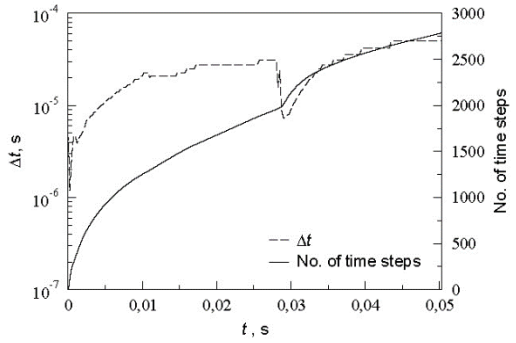

Slika 11. *Veličina vremenskog koraka i broj iteracija za proračun udara kapljice*
Figure 11. *Time step size and number of iterations for the computation of drop impact*

4. CONCLUSIONS

The algebraic volume-of-fluid model for interface capturing in free-surface flows in OpenFOAM® has been presented. The compressive scheme is specially devised to suppress the numerical diffusion and compress the smeared interface. The model potential is demonstrated by computing droplet shape evolution free of gravity and drop impact onto a liquid wall-film. According to the simulation results the model shows good capabilities for the simulation and prediction of free-surface flows.

5. REFERENCES

[1] D. Gerlach, G. Tomar, G. Biswas, and F. Durst: *Comparison of volume-of-fluid methods for surface tension-dominant two-phase flows*, International Journal of Heat and Mass Transfer, 49:740-754, 2006.

[2] A. Albadawi, D.B. Donoghue, A.J. Robinson, D.B. Murray, Y.M.C. Delaure: *On the assessment of a VOF based compressive interface capturing scheme for the analysis of bubble impact on and bounce from a flat horizontal surface*, International Journal of Multiphase Flow 65:82-97, 2014.

[3] P. Cifani, W.R. Michalek, G.J.M. Priems, J.G.M. Kuerten, C.W.M. van der Geld, B.J. Geurts: *A comparison between the surface compression method and an interface reconstruction method for the VOF approach*, Computers and Fluids, 136:421-435, 2016.

[4] OpenFOAM® The open source CFD toolbox, https://www.openfoam.com/

[5] J.U. Brackbill, D.B. Kothe, and C. Zemach: *A continuum method for modeling surface tension*, Journal of Computational Physics, 100:335-354, 1992.

4. ZAKLJUČCI

Predstavljen je algebarski volume-of-fluid model za praćenje međufazne površine u toku sa slobodnom površinom u softveru OpenFOAM®. Posebno osmišljena kompresivna shema služi za smanjenje numeričke difuzije i kompresiju razmazane slobodne površine. Potencijal modela je predstavljen računanjem evolucije oblika kapljice bez gravitacije i udara kapljice u tečni film. Prema rezultatima simulacije model pokazuje dobre sposobnosti za simulaciju i predviđanje tokova sa slobodnim površinama.

[6] H.G. Weller: *A New Approach to VOF-based Interface Capturing Methods for Incompressible and Compressible Flow*, Technical Report TR/HGW/04, OpenCFD, 2008.

[7] H. Jasak, H.G. Weller, and A.D. Gosman: *High resolution NVD differencing scheme for arbitrarily unstructured meshes*, International Journal for Numerical Methods in Fluids, 31:431-449, 1999.

[8] H. Rusche: *Computational fluid dynamics of dispersed two-phase flows at high phase fractions*, PhD thesis, Imperial College of Science, Technology and Medicine, London, 2002.

[9] E. Berberovic, N.P. van Hinsberg, S. Jakirlic, I.V. Roisman, and C. Tropea: *Drop impact onto a liquid layer: Dynamics of the cavity evolution*, Physical Review E, 79:036306, 2009.

Coresponding author:
Edin Berberović
Polytechnic Faculty, University of Zenica
Email: eberberovic@ptf.unze.ba
Phone: +387 32 449120